

Trade Studies in Multi/hyperspectral Imaging Systems

Final Report

Pantazis Mouroulis, David A. Thomas, Thomas G. Chrien, Valerie Duval, Robert O. Green, John J. Simmonds, Arthur H. Vaughan

Jet Propulsion Laboratory

10/29/98

Contents

Introduction

I. First-order requirements and basic system architecture trades

1. Type of scan
2. Spectral sampling

II. Detailed specifications and calibration requirements

1. Spectral requirements
2. Radiometric requirements
3. Spatial requirements
4. Measurement requirements conclusion

III. Examples of point designs

1. A system with 130 km swath, 30 m ground spot size
2. A high-SNR system for local/regional research
3. A 120° FOV system for global coverage
4. A hyperspectral system for the thermal IR

IV. Technology advances

1. Progress in spectrometer optical design
2. Progress in dispersive element fabrication
3. Progress and issues in focal plane arrays
4. Progress and issues in silicon carbide technology
5. Progress and issues in fiber optics
6. Summary of important technology issues

V. Conclusions

References

Trade Studies in Multi/hyperspectral Imaging Systems

Final Report

Introduction

This report is concerned with Earth-observing systems, operating in the solar reflected spectrum, and from Low Earth Orbit. It addresses the following issues:

- specifications of multi/hyperspectral imaging systems that address current science needs and enable new science and applications
- examples of point designs that satisfy the above requirements and specifications
- technology advances needed to reduce above systems to practice

The applications addressed through such systems are in the areas of Land Cover and Land Use Change, Natural Hazards Research, and Atmospheric and Ocean Monitoring. Within those areas, several possible applications are served such as mineral exploration, cloud cover and atmospheric moisture, hazardous waste monitoring and cleanup, agricultural crop status and yield, forest fires and regrowth, forest health, urban monitoring and planning, wetland monitoring, ocean plankton, coastal area monitoring, etc.

I. First-order requirements and basic system architecture trades.

The above applications require two distinct classes of imaging systems, depending on the necessary ground resolution (GSD) and field of view (FOV) coverage. The first class of systems has a 10-30m GSD, for regional to local scale science research. A typical FOV or swath for such a system is in the few tens of km. The second class of systems requires a GSD of about 1 km and a very wide FOV (corresponding to ~1000 pixels) for global coverage. In between these two types is a system with 30 m GSD with a ~160 km FOV for Landsat-type coverage.

There are two fundamental trades for these systems that involve a) the basic system architecture (type of scan) for sufficient signal-to-noise ratio (SNR), and b) the required spectral sampling or resolution and its impact on system architecture (multi- or hyperspectral system).

1) Type of scan

There are three distinct scan methods for acquiring an image. The first two (whiskbroom and pushbroom) are adequately described in the literature. From our viewpoint, the whiskbroom system has the simplest calibration requirement and derives the purest spectra since there is only a linear detector array, and the spectrum of every point on the ground is recorded by that single array. However, whiskbroom systems do not have adequate SNR from space due to the limited integration time. The pushbroom scan offers the highest SNR, but at the expense of some nonuniformity and calibration difficulties introduced by the need to characterize many different detector arrays, the number of which equals the number of spatial pixels. Nonuniformity is introduced across the FOV by two sources. The first is due to variations in the response of the detector array. Although gross variations in response may be corrected with a gain calibration, minor errors in the calibration, such as those related to detector non-linear response, will cause striping in the data. The second source of non-uniformity is variation in the spectral response function of the spectrometer across the field of view. These variations can not be corrected with

calibration due to the high frequency spectral detail imparted by atmospheric transmittance. Unlike the whiskbroom scan which requires a constantly moving scan mirror in order to cover the entire FOV, the pushbroom system needs no moving parts (assuming pointing is accomplished by the platform motion).

The third type of scan, called time-delay integration (TDI), is a hybrid type that attempts to combine some of the advantages of both pushbroom and whiskbroom scans. A scanning mechanism is used in conjunction with a pushbroom imaging spectrometer, but the scan is such that every pushbroom sample observes every spatial IFOV of the ground. A straightforward implementation of this concept is to scan along the pushbroom slit instead of the conventional perpendicular to slit scan; this may be called a knife-edge scan to differentiate it from a pushbroom scan. Another scanning scheme is to pushbroom scan perpendicular to the spacecraft velocity vector at a rate that progresses one pushbroom sample per scan period.

Every sample along the knife edge or cross-track pushbroom observes the same point on the ground but at different, sequential times. A time delay scheme is then used to align these samples. The result, after alignment is multiple looks at the same point on the ground. These multiple samples increase the signal to noise ratio over a single look. Non-uniformity across the slit is effectively eliminated since all spatial pixels will be composed of the same sum of non-uniform samples. The summing may be done either before or after digitization. If done before digitization, such as on a TDI CCD array, then a N times increase in SNR is achieved, where N is the number of samples along the slit. This scheme works in the knife-edge scan mode only. If the summing is performed after digitization than only a \sqrt{N} increase in SNR is achieved. This design approach relies on access to TDI focal planes, or very fast digital signal chains for summing, and trade-offs which involve available detectors become pertinent.

The advantages of this type of scan are the increased SNR relative to a whiskbroom system, and improved spectral fidelity (see below) relative to a pushbroom system. The disadvantages are a reduced SNR relative to a pushbroom system and the reliance on a moving mirror scan. With respect to the foreoptics, the TDI system reduces the need for a wide simultaneous FOV by a factor of four or greater, but must use a lower f-number for high SNR, as well as a longer focal length to accommodate larger pixels. Because this is an unusual architecture, we have generated a comparison chart to show the SNR of some candidate systems. The SNR shown in the chart below represents an approximate band average, with the SNR of a pushbroom system normalized to unity for comparison purposes. A linear increase in SNR with N has been assumed.

	Pushbroom 800 pixel swath 27 μm pixel f/4	64x TDI 2048 pixel swath 60 μm pixel f/1.8	64x TDI 2048 pixel swath 40 μm pixel f/1.8	128x TDI 2048 pixel swath 40 μm pixel f/1.8
VNIR	1	0.78	0.50	0.72
SWIR	1	0.77	0.49	0.72

A TDI factor of 64 and possibly of 128 are considered achievable at this point. At higher factors, timing errors between the readout and the scan mirror become noticeable. While the TDI system may prove to be the best solution for specific applications, for the purpose of this report we concentrate on pushbroom systems and on methods for improving their spectral fidelity/uniformity characteristics, as well as the FOV without the use of moving parts.

2) Spectral sampling

Several applications documented in the literature have demonstrated the need for and benefits of hyperspectral systems with a typical sampling interval of 10 nm over the 400-2500 nm band. Such systems not only permit accurate identification of ground samples due to the detailed spectral signatures they collect, but also allow for correction of the effects of the atmosphere without the use of a separate atmospheric sounder. This spectral resolution is not needed for all applications. In a few cases, a multispectral system with 10-12 bands suffices. A filter-based implementation of such a system leads to either complicated beam splitting arrangements for simultaneous recording of all spectra, or moving filter wheels.

Progress in spectrometer design and fabrication detailed below has now made such multispectral systems look cumbersome. It is possible to design highly compact spectrometer forms with high efficiency gratings tailored to a variety of FPA formats. Generally, a low-dispersion spectrometer would compare favorably with a multiple filter arrangement in practically every possible aspect, including mass, volume, number of parts, simplicity, and reliability. Therefore, for the purposes of this study we have concentrated on hyperspectral systems with the understanding that a multispectral design is similar but simpler due to the reduced dispersion.

II. Detailed specifications and calibration requirements

The primary measurement requirements for the instruments of concern may be viewed in terms of spectral, radiometric and spatial characteristics. Within each category, we address the following properties: range, sampling, response, stability, uniformity, precision and accuracy.

1) Spectral Requirements

The basis for many of the spectral requirements for imaging spectrometers operating in the solar reflected spectrum comes from the nature of the upwelling spectral radiance arriving at the sensor. The upwelling spectral radiance is dominated by narrow absorptions induced by the molecules in the Earth's atmosphere (Figure 1). The data measured by an imaging spectrometer result from the convolution of the upwelling spectral radiance with the spectral channel sampling and response function of the sensor. Errors in the knowledge of the spectral position and spectral response functions induce large errors in the measured radiance (Figure 2). These errors mimic and distort the spectral signatures of materials that are targeted by imaging spectrometers. The need to avoid these errors drives the spectral requirements described below.

Range: Measurements with laboratory spectrometers, field spectrometers and airborne imaging spectrometers have shown that spectral sampling from 400 to 2500 nm enables a range of science research and applications (Green, et al. 1998a).

Sampling: The spectral absorption and scattering characteristics of the range of liquid and solid materials found on the Earth's surface are well recorded with spectral sampling of 10 to 20 nm.

Response: A spectral response full width at half maximum (FWHM) of 10 to 20 nm matching the sampling is sufficient to record the spectral absorption and scattering characteristics of the range of liquid and solid materials found on the Earth's surface. Advantages arise if the spectral response function has an easily modeled form such as Gaussian.

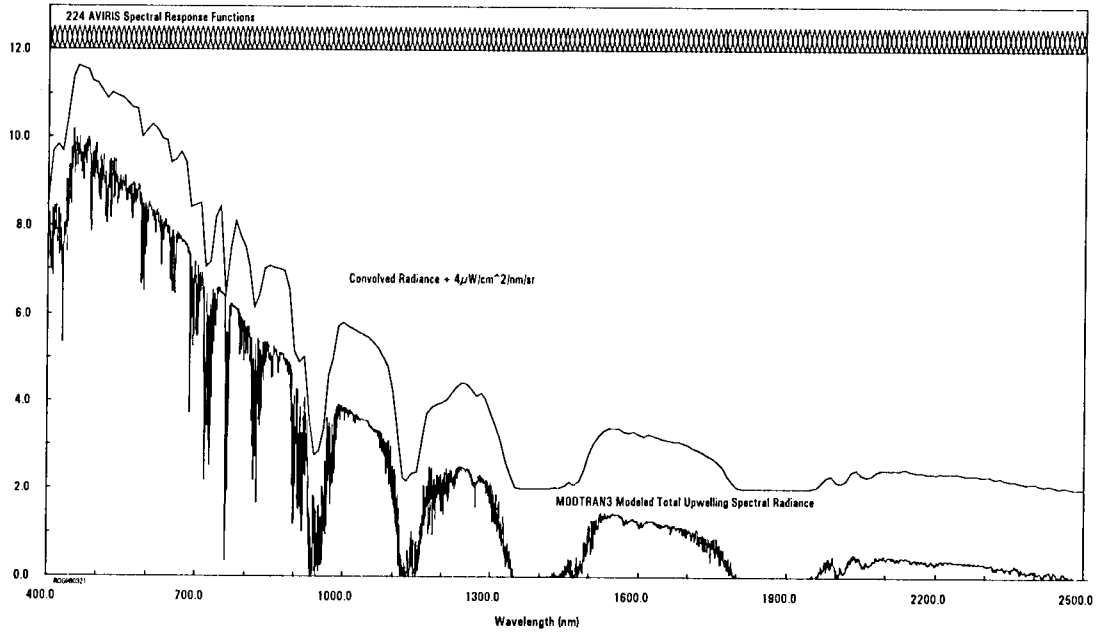


Figure 1. Model and convolved upwelling spectral radiance for an imaging spectrometer.

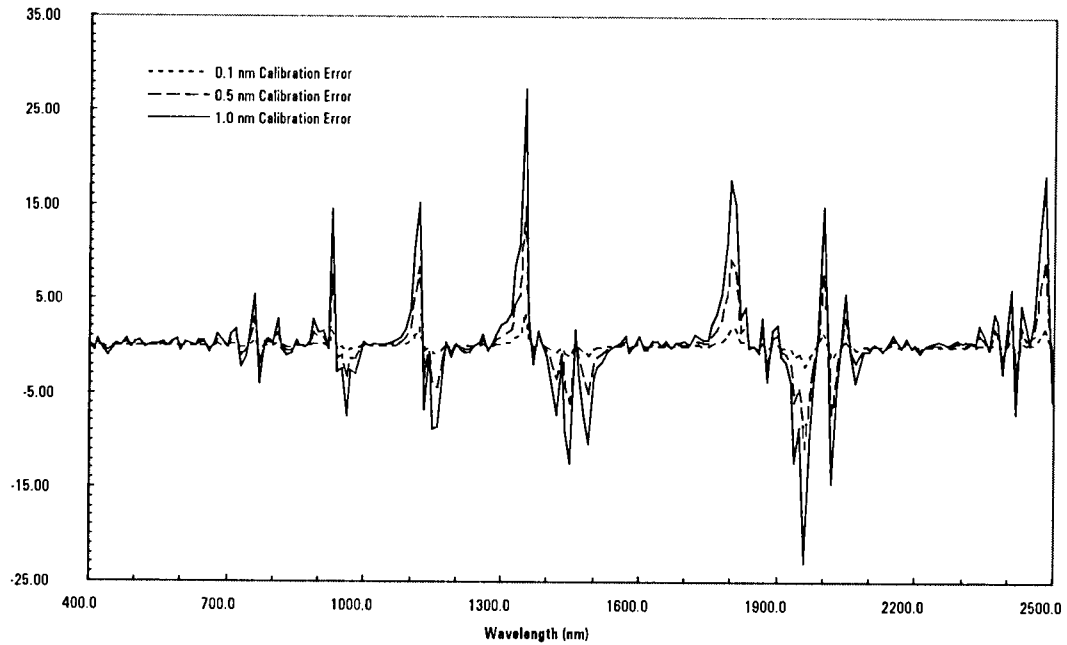


Figure 2. Error induced in measured radiance due to error in knowledge of spectral channel position.

Response and sampling: Ideally, the spectral sampling of the imaging spectrometer would be at half the interval of the response function. Current practical systems have sampling equal to the interval of the response function.

Stability: Stability is viewed as the variation of spectral channel position and response function between different image acquisitions. At the highest level, a sensitivity analysis has been performed on the requirement for spectral calibration for imaging spectrometers in this portion of the electromagnetic spectrum (Green 1998b). This work shows a baseline requirement of 3% and a goal of 1 % for error in knowledge of spectral calibration. If the spectral calibration may be determined independently for each image acquisition, then the stability requirement may be loosened.

Uniformity: Uniformity is viewed as the known variation in spectral sampling and spectral response throughout an image. A requirement of 3% and goal of 1% is derived from the spectral calibration sensitivity analysis (Green 1998b). For a pushbroom sensor, this requirement translates into a specification for the so-called 'smile' or spectral distortion to remain below the 3% pixel level.

Precision: Spectral precision is viewed as the unknown variation in spectral sampling and spectral response throughout an image. Because this is expressed as an error in calibration the requirement is 3% with a 1% goal (Green 1998b).

Accuracy: This is considered to be the knowledge of the spectral position and response function of all spectral channels.

2) Radiometric requirements

Range: A nominal radiometric range requirement for imaging spectrometers in the solar reflected spectrum is from 0 to maximum Lambertian reflected radiance (Figure 3). The range is appropriate for almost all Earth materials. The exceptions are hot targets such as fires and specular targets such aluminum roofs or water at low zenith illumination.

Sampling: To measure radiances of dark targets such as vegetation in the visible portion of the spectrum or water targets, a sampling interval of equal to or less than $0.05 \mu\text{W}/\text{cm}^2/\text{nm}/\text{sr}$ is required. This leads to a requirement of 12 bits of digitization or greater.

Response: The radiometric response of the imaging spectrometer should be linear or known. Linear systems are easier to characterize and calibrate.

Stability: Radiometric stability is viewed as the variation in radiometric sampling and response from image to image. To achieve calibration accuracy approaching 1% the stability should approach 1%. On-board calibration may be used as a strategy to bring relative radiometric knowledge to the 1% level, however, on board calibrators may themselves vary through time.

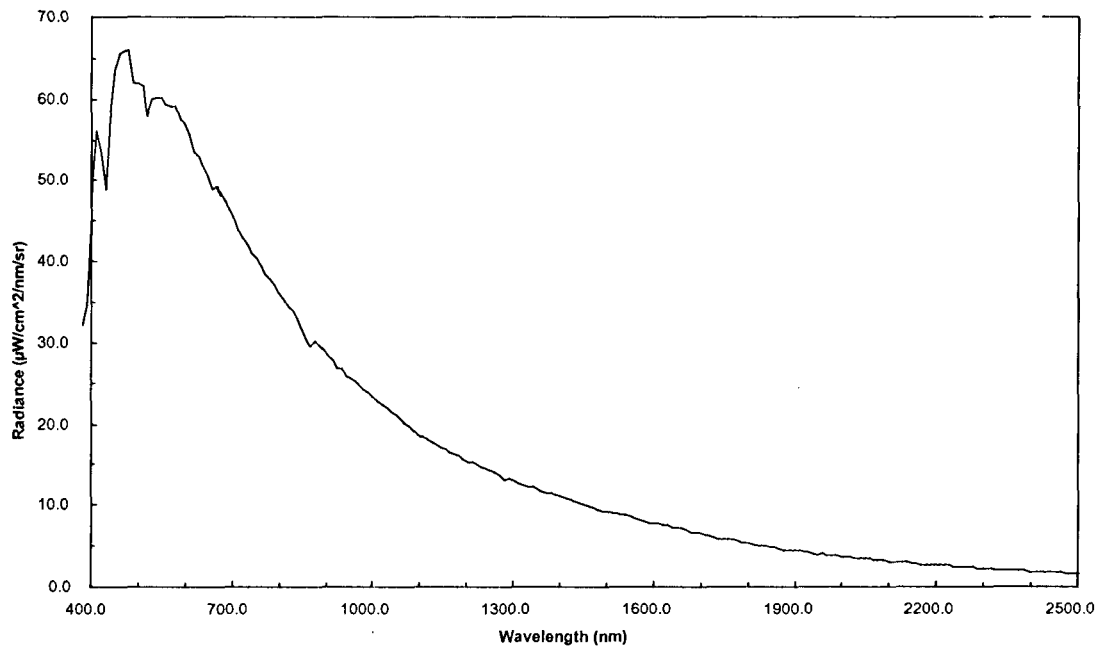


Figure 3. Maximum Lambertian reflected radiance.

Uniformity: Radiometric uniformity refers to the variation in radiometric sampling and response throughout an image. The more uniform the system, the more easily characterized and calibrated. Variation in uniformity may be accepted only to the level it may be measured and compensated close to the 1% level. Uncompensated non-uniformity accrues directly as radiometric calibration error.

Precision: Radiometric precision refers to the variation in consecutive measurements of the same target. This may also be referred to as signal-to-noise ratio or noise equivalent delta radiance. The desire to measure the spectral properties of dark materials such as water and vegetation in the visible portion of the spectrum coupled with the desire to make measurements under a range of illumination conditions drives the precision requirement. For a 25% reflectance target and 45° solar zenith angle, a peak SNR of 500:1 for the reflected radiance (Figure 4, 5) in each of the continuum regions is required. This SNR enables use of the full range of current analysis algorithms developed for airborne imaging spectrometers.

Accuracy: Radiometric accuracy is the relation between the reported radiance and the actual radiance. Current systems are exceeding 5% absolute radiometric accuracy. To recover spectral signatures from pixels containing spectra of multiple materials an accuracy of better than 1% is needed. Currently, “bootstrap” methods are used to achieve better than 1% effective accuracy. These methods often involve acquisition of ground measurements and forcing agreement with the imaging spectrometer data for the ground targets. To move beyond these “bootstrap” methods, a radiometric calibration accuracy approaching 1% is required.

3) Spatial requirements

Range (swath width or FOV): There are two classes of imaging spectrometer to consider. The first has a spatial range or swath width of 30-50 km and is appropriate for regional to local scale science research and applications. The second has a spatial range of ~1000 km and is appropriate for global imaging spectroscopy investigations.

Sampling (IFOV or GSD): The spatial sampling requirement for the first class of imaging spectrometer is 30 meters in the cross- and the along-track directions. This requirement is traced to the Landsat Thematic Mapper and is in effect required by the broad remote sensing community. Examples of such systems are the NMP-EO1 Hyperion, the Air Force's Warfighter and the Navy's NEMO. The second class of imaging spectrometer for global research requires spatial resolution on the 1000 m scale in the cross and along track directions. This enables the global coverage and is consistent with the current suite of global sensors (MODIS, AVHRR).

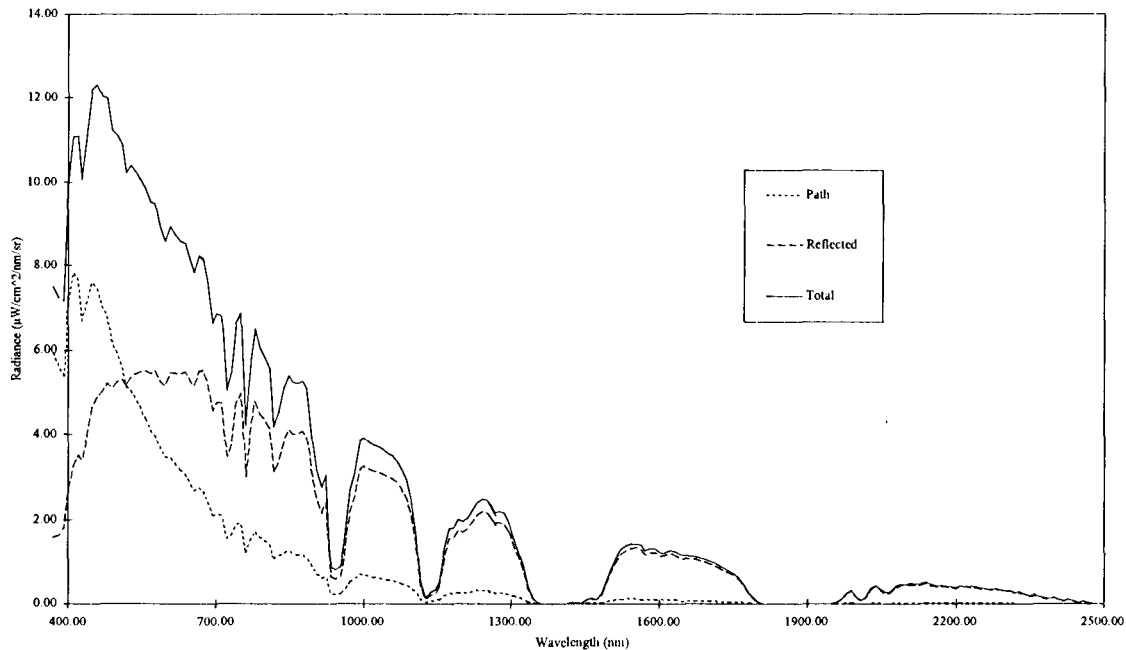


Figure 4. Radiance from a 0.25 reflectance surface illuminated from 45° solar zenith. The atmospheric path, surface reflected, and total radiance arriving at the sensor are shown.

Response: For both classes of imaging spectrometers the spatial response function width must be comparable with the spatial sampling.

Sampling and Response: As with the spectral domain, an oversampled spatial image would enable more robust resampling and sub-spatial element detection. However, oversampling by a factor of 2 increases the data rate by a factor of 4 and is likely not practical. There is also a physical limit on array size that then limits the number of spatial pixels that can fit into a single array.

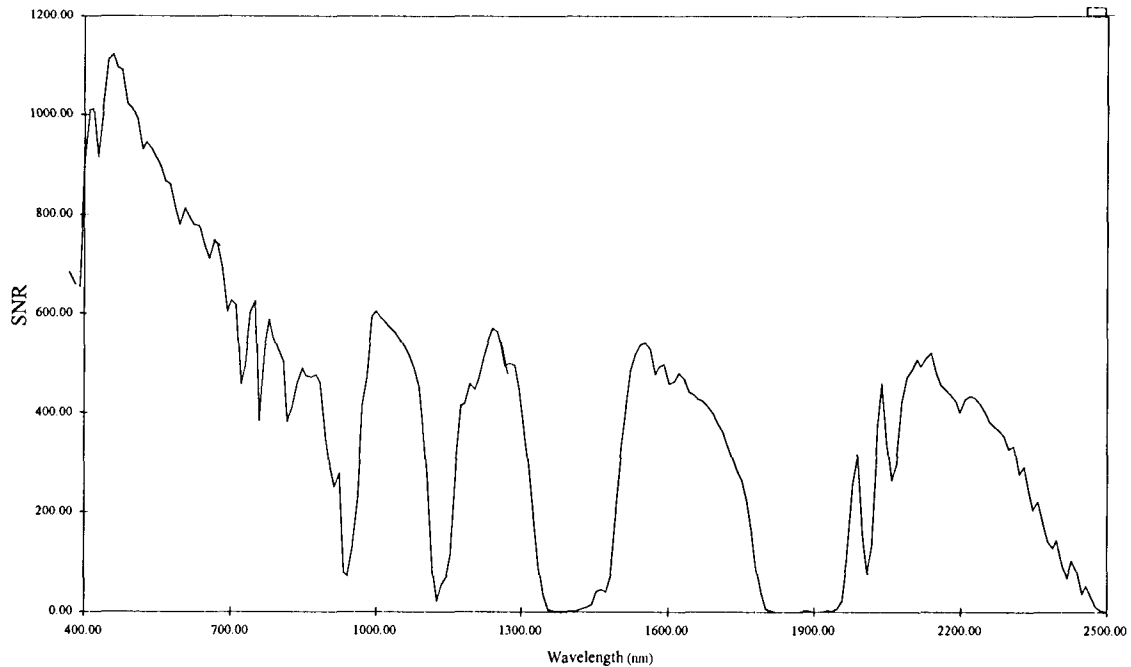


Figure 5. Signal-to-noise requirement for an imaging spectrometer in the solar reflected spectrum. This requirement is based on reaching 500:1 signal-to-noise for the reflected radiance component of the total radiance in each of the continuous regions of the spectrum.

Uniformity: Spatial uniformity refers to the variation of the spatial sampling and response of the imaging spectrometer throughout the image. Complete uniformity allows every measurement to be compared directly with every other measurement in the image. Uniform systems are much more straightforward to calibrate and hence utilize. A spatial uniformity requirement of 5% is reasonable. The second class of global imaging spectrometers will likely have spatial sampling and response variation across the swath. This variation must be calibrated and known to the 5% level.

Stability: Spatial stability refers to the repeatability of the spatial range, sampling, and response from image to image. Spatial stability is required at the 5% level to enable comparison of derived material concentrations for region to region and from time to time. If the spatial properties are not stable, then the requirement is to determine the properties to the 5% level for rigorous science research and application objectives.

Uniformity spatial and spectral: A special class of spatial and spectral uniformity requirement arises in the context of current set of proposed spaceborne imaging spectrometers. This requirement is that the spatial sampling and response not vary by more than 5% across the spectral range. In other words, all the wavelengths of the spectrum must come from the same place on the ground at the 95% level. If the spatial sampling and response vary as a function of wavelength, large errors in radiance and derived reflectance are induced (Figure 6 and Figure 7). More important than the large errors is the result that the spectra are not physically real. In one part of the spectrum one material is measured and in another part of the spectrum another material is measured. Such spectra will compromise the current suite of anomaly detection and imaging spectroscopy analysis algorithms, because the observed spectra are not represented in any spectral

library. Note: It might be possible to compensate for this error if the data are oversampled in the spatial dimension by a factor of 2 or more. However the data rate, volume, and processing overhead is large.

Precision: Spatial precision refers to the variation of spatial sampling and response expressed from consecutive measurements of the same target. The baseline requirement is that the spatial sampling and response not vary in an undetermined manner by more than 5 % in an image.

Accuracy: Spatial accuracy is the calibration knowledge of the spatial range, sampling, and response of the imaging spectrometer. Currently spatial information is rarely used to quantify the expressed concentration of materials at subpixel resolution. However, in the future, as spectroscopic analysis is applied to imaging spectrometer data, issues of expressed areal concentration will become important. This increased analysis burden drives the spatial accuracy requirement the 5% level. In the distant future this requirement may be pushed to the 1% level.

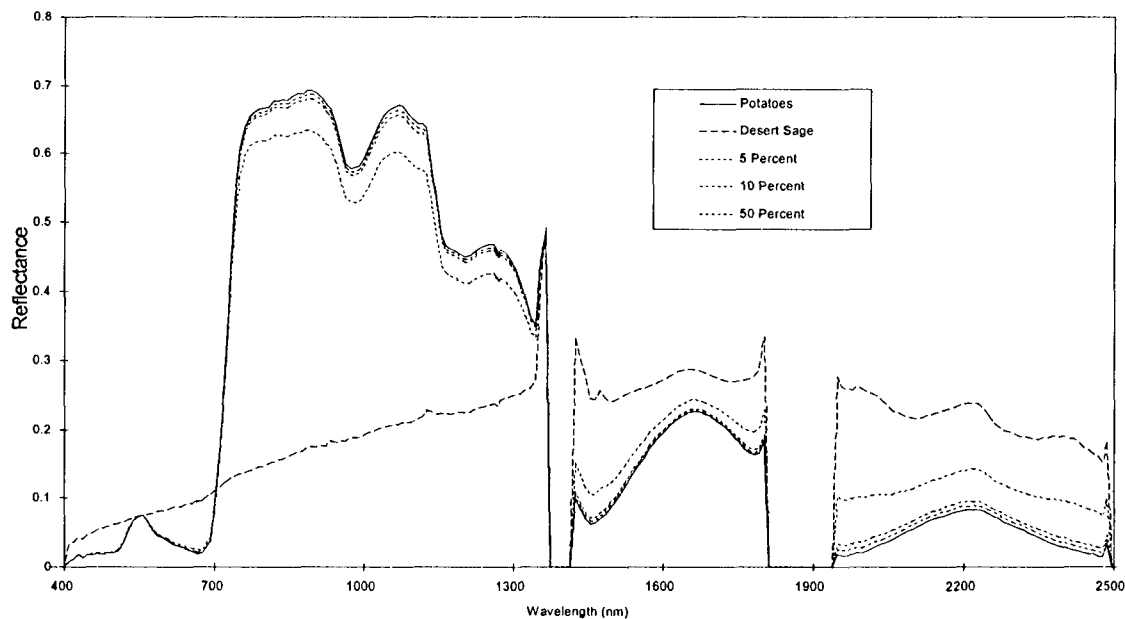


Figure 6. Measured reflectance spectrum of a potato field and adjacent area of desert sage. Based on the two pure spectra, spatial/spectral mixtures rising to 5, 10 and 50 % from 400 to 2500 nm are calculated to simulate spatial nonuniformity. The error is assumed to increase linearly as a function of wavelength, simulating 'keystone' or an increase in the extent of the optical point spread function (see Sec. IV.1 for explanation of terms). For short wavelengths, the spectra originate from the same patch of ground, containing only one vegetation spectrum. At the 2500 nm wavelength end, the spectra originate from a patch of ground that contains mixture of the two vegetations in the percentage noted. Thus the overall recorded spectrum is not physically realizable.

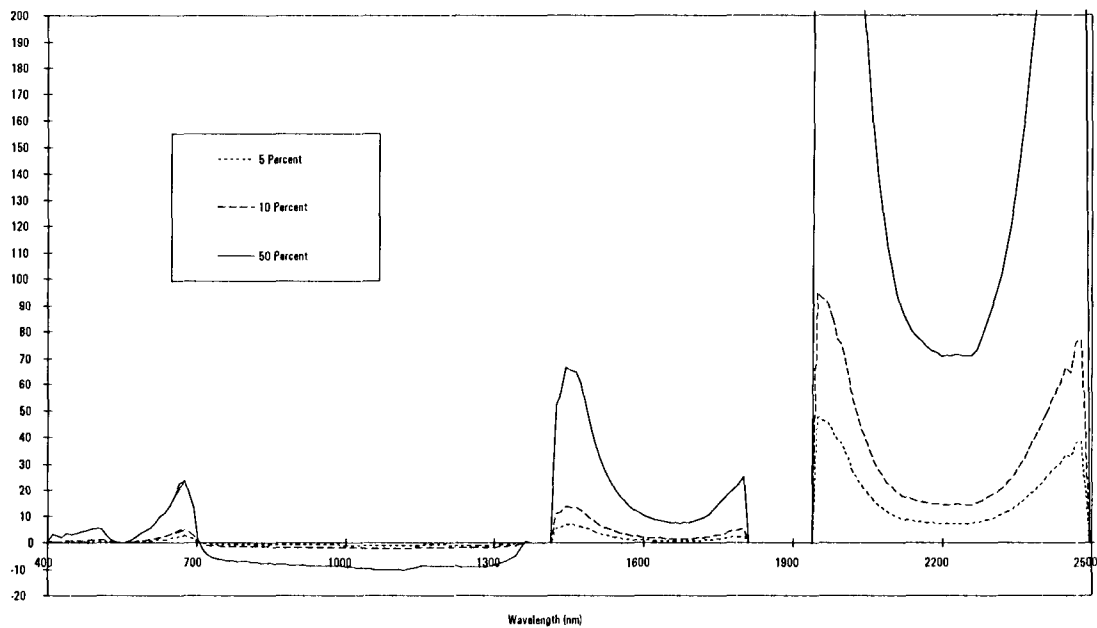


Figure 7. The percent error in reflectance as a function of changing spatial sampling and response as a function of wavelength.

4. Measurement requirement conclusion

Spaceborne imaging spectrometers are being developed to measure the solar reflected upwelling radiance spectrum from 400 to 2500 nm at 10 nm resolution. The objectives of these imaging spectrometers are to use the molecular absorptions and constituent scattering characteristics expressed in the spectrum to: 1) detect and identify the surface and atmospheric constituents present; 2) assess and measure the expressed constituent concentrations; 3) assign proportions to constituents in mixed spatial elements; 4) delineate spatial distribution of the constituents; 5) monitor changes in constituents through periodic data acquisitions; and 6) validate, constrain and improve models. To achieve these results, imaging spectrometers must meet certain spectral, spatial, and radiometric requirements. An attempt has been made to specify the current best understanding of these measurement requirements for spaceborne imaging spectrometers in terms of the range, sampling, response, stability, uniformity, precision, and accuracy. In addition to the above objectives, the new requirements for calibration, uniformity, and stability enable comparisons between the observations made with different sensors at different times.

II. Examples of point designs

Four point designs are described in this section that have been conceived or developed at JPL. They all rely on novel forms of concentric imaging spectrometer modules and address different and distinct science needs. All designs represent major improvements in performance over current and planned hyperspectral imaging systems and promise a greatly enhanced science return. Because of photodetector response, the 400-2500 nm band is split into VNIR (400-1000 nm) and SWIR (1000-2500 nm) in all cases.

1. A system with 130 km swath, 30 m ground spot size

This system relies on a wide FOV (15°) unobscured front telescope and a bank of six miniature spectrometer modules sharing a long slit in order to achieve the large swath. Each spectrometer module comprises a VNIR and a SWIR spectrometer, each with 720 spatial pixels. The system achieves the specified swath from a 490 km orbit, however some variation in orbit and swath is possible by varying the front telescope focal length. It is possible also to scale the swath down by removing one or more spectrometer modules and also to increase it slightly by adding one more. The limitation in pixel size and number of pixels per spectrometer comes from the available choice in HgCdTe arrays. As focal plane technology advances, the system can progress toward a nominal 1000 spatial pixel per module, giving a system swath width comparable to Landsat. The f-number is 4.

The number of spectrometer modules may give the impression that this is an impossibly complex system. In fact, the architecture is simple: the light arrives at any one spectrometer after only two reflections from flat fold mirrors. This is accomplished by a field-sharing rather than an amplitude-sharing arrangement. Figure 8 shows the schematic, from which the spectrometers have been removed for clarity. The telescope is a three-mirror anastigmat (TMA) design (mirrors M1, M2, and M3). The direction of scan (or motion) is up, while the swath (or slit) is perpendicular to the paper. A two-sided mirror with an apex angle of $\sim 70^\circ$ is used to split the light towards the VNIR (up) and SWIR (down) bank of spectrometer modules. Thus the VNIR spectrometers see the same patch of ground a short time after the SWIR ones. A similar two-sided mirror splits the light into left and right within the SWIR and VNIR bands separately, so that three of the SWIR spectrometers are to the (bottom) left and three to the right, and similarly for the VNIR. The spectrometers are into the paper and only four would appear in this projection.

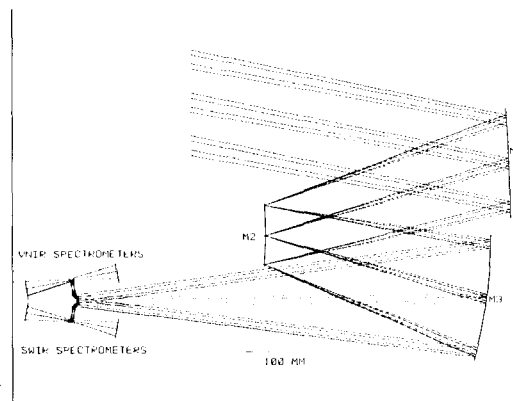


Figure 8. Schematic of telescope/beamsplitting arrangement (y-z section).

The system becomes feasible because of JPL's miniature Offner spectrometer design. This is shown in figures 9 and 10. The SWIR and VNIR modules can be made with identical optical prescriptions. Figure 9 shows the SWIR module along the spectral direction and figure 10 shows the module along the direction of the slit. In this latter projection, the slit and its image are coincident and appear identical because of the unity magnification of the spectrometer.

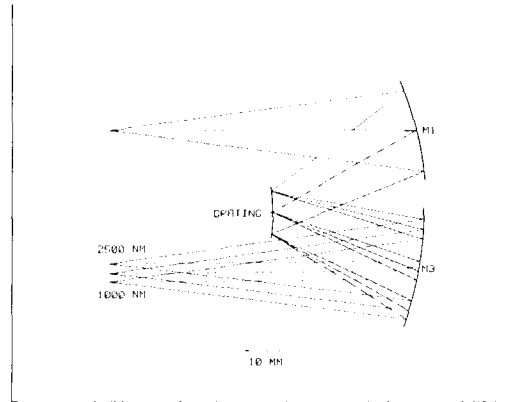


Figure 9. Miniature Offner spectrometer (y-z section).

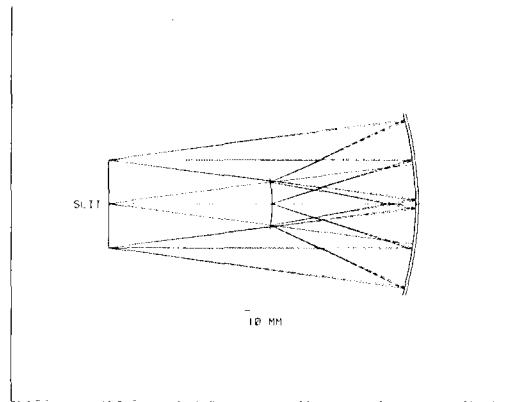


Figure 10. Miniature Offner spectrometer (x-z section)

It can be seen from Fig. 10 that the spectrometer modules have a height of less than twice the slit length. This makes it possible to stack them so as to share a longer slit without any further folding. It is therefore the combination of the field splitting arrangement with the spectrometer size that makes possible the simple architecture. A further advantage is that all focal planes can be arranged along the same plane (one for SWIR, one for VNIR) and with the minimum necessary distance between them. This is accomplished by one fold mirror in the output path (not shown in the figures) and has the effect of simplifying both FPA mounting and cooling arrangements.

Despite their small size, the spectrometer modules provide a high level of performance in terms of the requirements set forth in the previous section. While this is not the appropriate place for providing detailed performance calculations, we may note that they should be expected to

perform better than any pushbroom system to date in fulfilling most of the requirements set forth in Sec. II. Further, they employ only spherical concentric mirrors, and should be expected to approximate theoretical performance closely, as well as be easy to align and fabricate. This has been demonstrated with a breadboard of the system

Thus this architecture provides simultaneously high spatial and spectral resolution, over wide spectral range and a swath comparable to that of Landsat. And it does so using relatively simple optics, readily available detectors, no moving parts, and an all-reflective architecture that should provide maximum thermal stability.

The field splitting technique has two significant advantages: simplicity and high throughput since it avoids amplitude beamsplitters. It carries however a penalty in that the telescope must produce a zero-distortion image in order to have the same focal length across the VNIR and SWIR and avoid misregistration. Focal plane coregistration over such a wide FOV is probably the most important issue that would have to be addressed in a detailed design effort. Preliminary attempts have shown that it is possible to reduce the distortion of the telescope to less than a quarter pixel level even over the entire 15° FOV (or 4320 pixels). However, this necessitates the use of 6th order aspheric mirrors. The resulting additional complication in construction vs. the imperfect registration penalty would be part of a detailed design trade that has not been attempted to date.

It is also noted that the data rate of such an instrument will call for advanced transmission techniques such as the optical data link being developed at GSFC.

2. A high-SNR system for local/regional research

The previous design offers a wide field of view and a good SNR thanks to its f-number of 4 (this may be compared with the NM-E01 Hyperion spectrometer operating at f/11). However, it is unlikely that it can reach the peak SNR of 500 discussed in Sec. II 2. In order to achieve that high number, a significant increase in light gathering capacity is needed. The resulting low f-number means that a wide FOV is not simultaneously achievable. Nevertheless, a system with 700-1400 spatial pixels appears feasible.

The second point design is an f/1.3 system with 720 spatial pixels (18 μm) that can achieve a 15m ground resolution from a nominal 500 km orbit. This system again comprises separate VNIR and SWIR spectrometer modules. The front end telescope has sufficient FOV to support two modules in each band in a similar field-splitting arrangement as in the previous section, thus doubling the field of view if one retains the 15 m ground spot. Alternatively, the telescope may be scaled to provide a 30 m ground spot and an associated wider field for the same number of pixels.

The heart of this point design is the Dyson spectrometer, shown in figure 11. This is a remarkable design for its simplicity, compact size, and ability to handle such a low f-number. It has been designed as an f/1 system, but the limitation in the f/no of the point design comes from the telescope.

The Dyson spectrometer utilizes a large (several cm) concave grating. Here the grating is the largest element. All other refraction is accomplished by a single fused silica element with one side flat and another spherical. The input and output are nominally located on the flat side, but adequate clearance can be had for focal plane mounting. This consideration also implies that it is advantageous to use the alternative input location shown, by folding the input beam upwards. This is not shown here for simplicity. Figure 12 shows the x-z section where the slit can be seen.

This is also a unit magnification system, like the Offner, so the slit and its image are coincident in the x-z section. The slit has been placed just outside the flat silica surface.

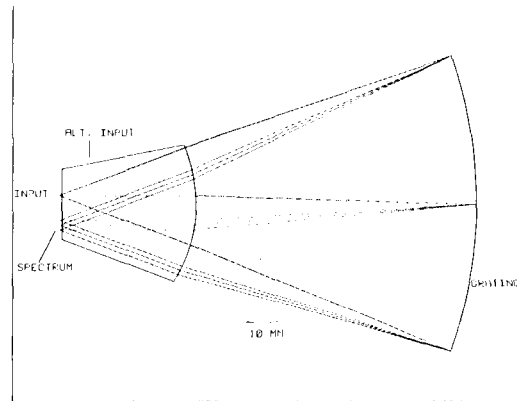


Figure 11. An f/1 spectrometer (y-z section)

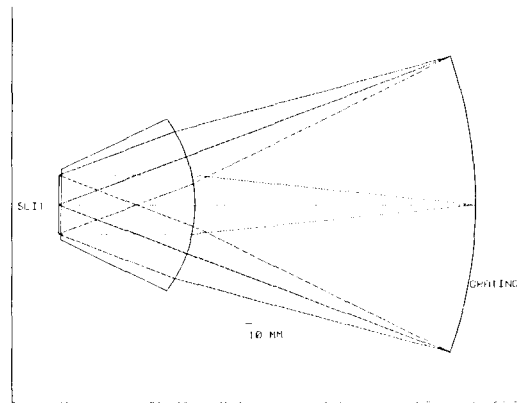


Figure 12. The f/1 Dyson spectrometer (x-z section)

The telescope design is shown in Fig. 13. While only a minimal amount of effort has been devoted to the task of designing the telescope, it was found possible to generate a three-mirror unobscured design with an f-number of 1.3 using no higher than 6th order aspheres. However, further reduction of the f-number from 1.3 to 1 may be difficult.

In summary, the second point design provides a high-SNR instrument with a very simple spectrometer design. The greatest part of the effort in this type of system would be directed towards fabrication and alignment of the front end telescope. Although this is not an all-reflective design, the concentric form of the spectrometer should provide for straightforward athermalization solutions.

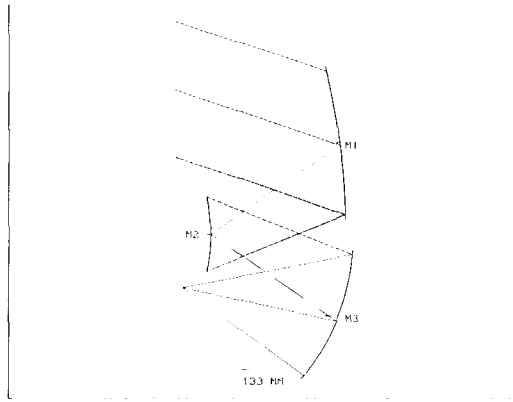


Figure 13. An unobscured telescope at $f/1.3$.

3. A 120° FOV system for global coverage

This system offers an ultra-wide FOV with a 2 mrad angular resolution. Used from a 500 km orbit, it provides a 1 km ground spot size. It has approximately 1024 resolvable elements. The heart of this type of system is in the foreoptic rather than the spectrometer design. In this case, the foreoptic is the smaller part of the system. When coupled with the compact Offner spectrometers described previously, the result is a true miniature optical system with unique capabilities.

The telescope comprises two simple mirrors one toroidal and one conical, that can be made easily through diamond turning techniques. The toroidal mirror focuses the beam in a way independent of field location, while the conical mirror acts essentially as a folding element to place the output beam axis perpendicular to the incoming one. The image of a line on the ground thus becomes an arc on the focal plane, with the size of the arc being the same as the angular FOV of the instrument (see Fig. 14). This curved image line is then populated with an array of optical fibers that can transmit the light to filters or spectrometers as desired. The system has an f/no of ~ 5 .

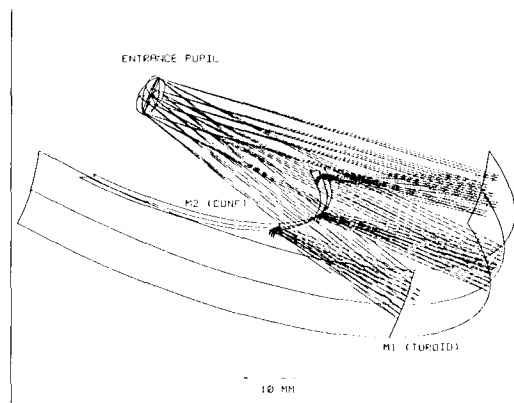


Figure 14. A 120° FOV telescope, shown here in 3-D view, with the 0°, 30°, and 60° beams.

In the implementation chosen here, the fibers reform the curved line into a straight one, that is then input to an Offner spectrometer as a slit. At least two adjacent layers of fibers must be used

in the telescope focal plane, one for the SWIR and one for the VNIR spectrometer. With available fibers, the total length of the resulting straight slit would be just over 6 cm. This cannot be covered by a single spectrometer. Taking into account the maximum size limitation for IR detectors, one of the following solutions would have to be adopted: i. The slit may be split into three spectrometers per band, ii. Two spectrometers per band may be used that slightly demagnify the slit to match the detector, iii. A slight reduction in FOV may be accepted so as to accommodate the entire slit into two unity magnification spectrometers.

The above trade represents one of the main design issues with this system, but it is a matter of engineering decision rather than technology development. Other design issues are associated with the nature of the fiber bundle that leaves small gaps in coverage due to the inactive area. This can be dealt with by using two layers of fiber per wavelength band, the second layer covering the gaps of the first. Another design issue concerns the fiber NA which is typically greater than that of the telescope, so the beam input to the spectrometer will likely have the NA of the fiber. This is not necessarily so because the short fiber length coupled with a relatively straight path may not allow a true equilibrium mode distribution to be established in the fiber. The optimum way of configuring the bundle will be a matter of some analysis and experiment.

Although this system relies on multiple spectrometer modules, the misregistration problem of the first point design is essentially absent. This is because the fibers decouple the telescope from the spectrometers, so each spectrometer acts independently. The Offner spectrometer modules were mentioned earlier and are also further discussed in the next section.

In summary, this is an extremely compact and powerful global coverage system with simple construction and an ultra-wide FOV.

4. A hyperspectral system for the thermal IR

Although for this trade study we chose to limit our investigations to the solar reflected spectrum up to ~2500 nm, the point design shown briefly in this section demonstrates that several of the concepts and techniques discussed earlier are applicable to longer wavelengths as well. This design operates in the 8.5 – 11.6 μm band with 64 spectral channels. It has a 30 m GSD and a 21.6 km swath from a 490 km orbit. Two Offner spectrometers are used, each with 360 spatial pixels. The f-number is 2.2 and the front telescope aperture is 445 mm. The FPA pixel size is 60 μm . The system schematic is shown in Fig. 15.

Due to the compact size of the Offner spectrometer, the telescope is by far the major contributor to size and mass in this design. More compact telescope designs of a similar aperture size are possible, but they suffer from various disadvantages which negate the smaller size. For example, an axial design with a central obscuration leads to a larger diffraction spread, which in turn requires larger pixel size and thus leads to fewer spatial pixels (smaller swath) for the same number of spectrometers. A more compact unobscured design necessitates a considerably more complicated spectrometer design. Like any point design, this one represents only a given set of choices from within the various possible system trades.

Unlike the previous hyperspectral systems that can perform atmospheric correction from the data they collect, this system requires a separate atmospheric sounder with higher spectral resolution over a limited band (and a much larger GSD). A sounder design also based on an Offner spectrometer has been generated, that occupies approximately the same volume as one of the spectrometers of Fig. 15.

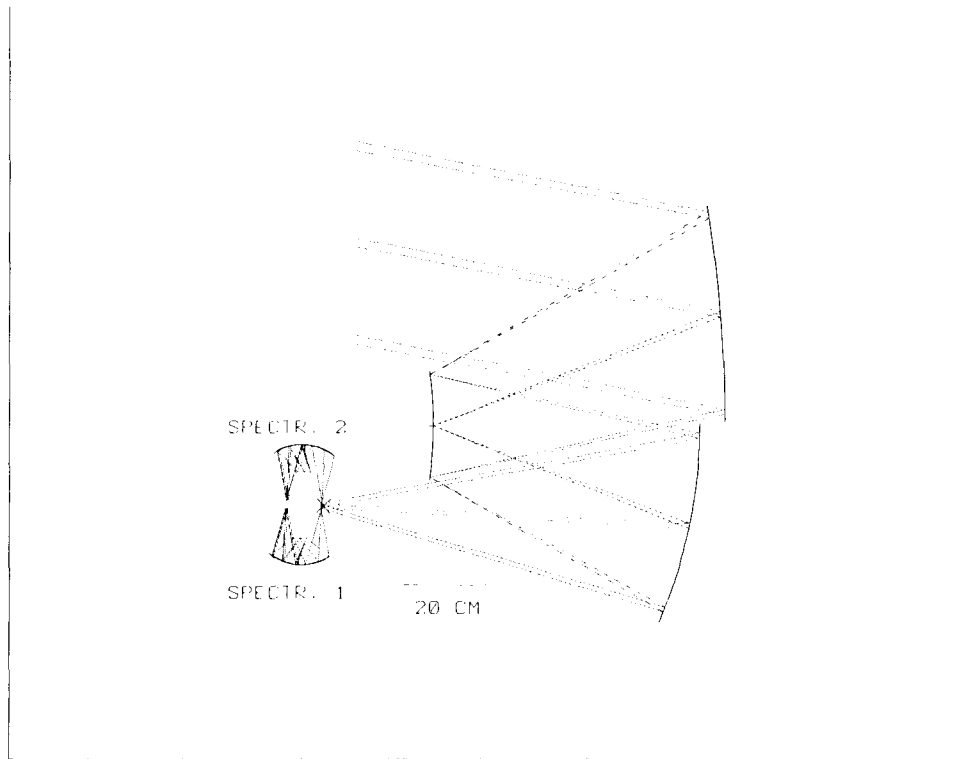


Figure 15. A thermal hyperspectral system

IV. Technology advances

This section identifies technologies that are critical for the implementation of the point designs of Sec. III. It is emphasized that all these systems are feasible even with current technology. The technology advances discussed here have to do primarily with performance optimization and with proving the systems in a space environment.

1. Progress in spectrometer optical design

The design of a pushbroom imaging spectrometer form that satisfies even approximately the requirements set forth in Sec. II of this report is a truly demanding task. Although considerable progress has been made to that end, a full investigation of all the possible design trades would be a matter of intense research effort over a period of approximately one year. However, even at the current state of development, the spectrometer forms that have been mentioned in Sec. III can already provide a level of performance that significantly exceeds any space-based system currently in operation and perhaps even in planning.

An appreciation of the complexity of the task can be had by translating the spectral and spatial calibration and uniformity requirements into optical parameters. This is done schematically in Fig. 16. The figure shows the ideal spectrum that a pushbroom imaging spectrometer must produce. The columns labelled "B", "G", and "R" represent the short, middle, and long wavelength slit images respectively. The spectrum of a point is obtained along a row. The filled circles or ellipses represent idealized optical Point Spread Functions (PSFs).

The following desirable optical characteristics are evident from the figure. All spectra are perfectly parallel between them and with the rows of the array. Similarly, the monochromatic slit image for any wavelength is perfectly straight and aligned with a column. In other words, the centroids of the PSFs form a perfect rectangle. This means that distortion must be absent. The width of the PSF (a or b) along any column also remains constant, though it is allowed to vary with wavelength. Finally, the height of the PSF (indicated by c) should remain constant, independent of wavelength, and also independent of spatial location.

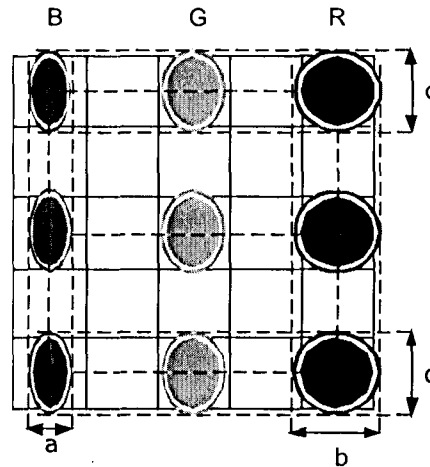


Figure 16. Schematic of spectrum produced by an ideal pushbroom imaging spectrometer

In practice, these conditions can only be satisfied approximately. A non-ideal spectrum that contains all possible errors is shown in Fig. 17. The figure shows the following errors.

- The “B” column exhibits a distortion that is called “smile”. This error will affect knowledge of the peak location of the pixel spectral response function.
- The “G” column shows variation in the width of the PSF. This error will affect knowledge of the FWHM or shape of the spectral response function.
- The top row is not aligned with the array, and when compared with the middle one shows that the spectrum is more like a trapezoid than a rectangle. This is called “keystone error” and affects the spatial uniformity requirement.
- The bottom row shows a PSF that increases in height with wavelength (as might be caused by diffraction). Although this may be inevitable in a diffraction-limited system, it nevertheless causes a spatial nonuniformity similar to the keystone error.

The tolerance for all the above errors is at the level of a small fraction of a pixel. From Sec. II, we see that the desirable level of control for the first two errors is $< \sim 2\%$, and for the last two $< \sim 5\%$ of a pixel.

Fortunately, there exist spectrometer forms that can minimize the above errors to a considerable degree while simultaneously offering a more compact size and simpler construction than past designs. These forms achieve their desirable characteristics by placing the grating on a spherical surface. They can also achieve very low distortion values because of their symmetric form. Although they have been in existence for some time, their potential has not been tapped.

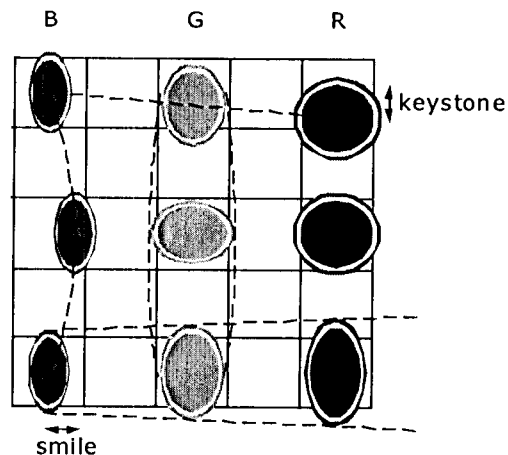


Figure 17: Schematic of errors by a non-ideal pushbroom imaging spectrometer

The first design form (Offner) is an all-reflective system with only three surfaces, two of which can sometimes be combined into a single element (used twice). A schematic of this system was shown in Figs. 9, 10. The following are the characteristics/advantages of the Offner spectrometer design with a convex grating as dispersive element.

- It accepts a long slit while maintaining a highly compact form. Several useful designs have been produced in which the maximum spectrometer dimension is only four to five times the slit length. Since the design is scalable, an absolute slit length specification is not particularly meaningful. However, designs with 25-27 mm slit length have been produced which make use of the maximum possible dimension in hybrid HgCdTe IR detector arrays (limited by detector/mux CTE mismatch).
- It provides negligibly small distortion (smile, keystone) if appropriately optimized.
- It can operate at relatively low f-number, greater than about $f/2.5$ for VNIR/SWIR applications. However, minimum size usually requires a higher f-number, of about 4.
- It has only three (two) optical surfaces (excluding fold mirrors not fundamental to the design form).
- It typically utilizes only spherical and centered surfaces. This feature, in addition to ease of fabrication and alignment, provides the best possible chance of approximating the theoretical performance in practice.

Several compact Offner spectrometer designs have been described by Mouroulis (1998) that present minimum smile and keystone errors of approximately 1% of a pixel. An experimental prototype has been described by Mouroulis and Thomas (1998), which achieves a smile level of 2% in practice.

The above does not exhaust the potential of the Offner design. For example, despite the small number of surfaces (and the associated small number of degrees of freedom) it is possible to produce Offner designs that present very small variation of the spectral response function with field. This generally needs a judicious balance between the size of the slit, the size of the pixel, and the size of the spectrometer. But in addition, the incorporation of an aberration-balancing function in the grating can be of help in reducing PSF variation with field. Such a development

represents a logical extension within the scope of current techniques, but one that would have to be tested in practice. In addition, it would be desirable to develop design optimization techniques based on explicit expressions of the requirements of Sec. II.

The second design form (Dyson) is again a three-surface nominally concentric design, but with surfaces 1 and 3 being necessarily identical (see Figs. 11, 12). This is the only simple design form demonstrated to date that can handle very low f-numbers for high SNR. The potential of this design has not been investigated in as much detail as that of the Offner to date, but representative designs of a VNIR and a SWIR module operating at $f/1$ with 720 spatial pixels and a 10 nm spectral sampling have been generated as shown in the previous section. These designs show also the low levels of smile and keystone that are possible with the Offner. Because the refractive surface is a possible source of ghosts, a first-order ghost analysis was performed which showed the necessity for a linear variable bandpass filter over the detector, a feature which has been tested in other imaging spectrometer designs.

The Dyson spectrometer is at a lower level of maturity than the Offner, but its simplicity should provide for a relatively low-risk development. It is clear that it has even fewer degrees of freedom than the Offner in controlling all the parameters necessary, but even in its simplest embodiment with two concentric spherical surfaces it provides a high level of performance. An associated non-trivial problem is the development of unobscured telescopes that can match the f-number of the Dyson, as noted earlier.

2. Progress in dispersive element fabrication

This section concentrates on diffraction gratings, which are the dispersive elements of choice for hyperspectral pushbroom imagers. The justification for this choice is as follows:

Dispersive elements can be divided into passive and active. The first category includes gratings, prisms and thin-film optical filters, and the second includes acousto-optic or liquid crystal tunable filters. The passive type is clearly preferable in terms of reliability and simplicity. Among the passive types, gratings and prisms can be readily employed for hyperspectral resolution (~ 10 nm). A hyperspectral sensor can also be constructed with a variable linear filter (LVF or wedge). However, a resolution of 10 nm is extremely demanding for a LVF in the long wavelength regime, as it would imply a bandpass of less than 1%. Also, practical limitations on system scan stability limit the usefulness of systems that do not simultaneously sample all spectral channels. The production, characterization, and calibration of an imaging spectrometer based on such a filter is still in the future.

On the other hand, grating and prism-based spectrometers are better understood. Generally, a prism has the advantage of uniformly high efficiency and low scatter. But optical designs based on prisms tend to be considerably more complex than their grating-based counterparts. Gratings permit the realization of all-reflective optical systems, as well as the exploitation of the considerable advantages of concentric spectrometer forms as explained in the previous section. In addition, peak efficiencies of $\sim 85\%$ are now achievable and the level of scatter that can be achieved is currently $< 0.1\%$, which rivals the level caused by imperfect coatings on prism surfaces.

There are two grating forms of interest, both formed on spherical (or nominally spherical) substrates. The first form is the convex grating type utilized in the Offner spectrometer and its derivatives. Gratings of this type tend to be small, typically 1" in diameter. The second form is the concave grating utilized in the Dyson spectrometer. In this case, the grating is the largest

element of the spectrometer, and it can have a diameter of up to 3-4", depending on the desired f-number. The size difference between the two forms leads to different technologies for grating production.

At this time, electron-beam (E-beam) grating production is rapidly becoming the technology of choice for the convex gratings of the Offner spectrometer. These gratings are scheduled to fly on the NMP-EO1 Hyperion and the AFRL Warfighter-1 instruments. The properties of these gratings have been investigated in some detail (Mouroulis et al, 1998). We give here a brief summary of the relevant characteristics.

The grating relief pattern is formed on a thin (~2 μm) layer of PMMA which is spin-coated onto the curved substrate. A reflective Al layer (30 – 50 nm thick) is evaporated on top. Adhesion, thermal cycling, vibration, and outgassing tests have been successfully performed as part of flight qualification.

These gratings can achieve the maximum possible efficiency under any desired spectral response specification. This is because the E-beam technique affords the flexibility of either varying the blaze angle or of keeping it constant across the extent of the grating. Typically, a blazed grating has the highest possible peak efficiency, but may not be adequate at short or at long wavelengths, depending on the width of the desired band. By varying the blaze angle, a broader band can be covered at the expense of peak efficiency. Since the E-beam technique generates the blaze angle of each groove independently by varying the exposure, it is possible to tailor the blaze angle variation to achieve a desired grating spectral response. In addition, coherence can be maintained from one groove to the next or from one panel to the next, unlike ruled gratings which normally show random or uncontrolled phase shifts between panels or areas with different blaze angles. Figure 18 shows an atomic force microscope scan of a dual panel (dual blaze) E-beam grating at the blaze boundary. The high quality of the grooves is evident. A small "picket fence" discontinuity is seen at the boundary due to imperfect pattern matching, however this is a small defect that does not affect the grating performance in any appreciable manner.

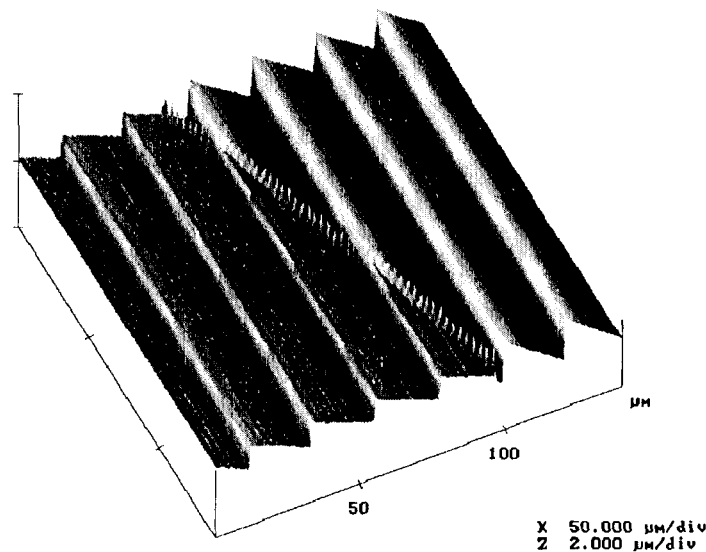


Figure 18. AFM scan of a dual blaze grating boundary

A relative peak efficiency of 88-93% in the first order has been consistently achieved for a single-blaze grating or grating panel. In addition to maximizing efficiency, the E-beam technique affords flexibility in constructing aberration-correcting gratings, or gratings with profiles that differ from the blazed sawtooth type for the purpose of obtaining a specified response. Further, in terms of achieving the design values of smile and keystone, there are two critical characteristics of these gratings, which cannot be achieved through ruling techniques. These are 1) that the phase shift between panels or different blaze areas is controllable, and 2) that the blaze areas (if more than one) can be made concentric, which minimizes the impact of intensity apodization on the location of the centroid of the PSF and hence on distortion.

E-beam gratings have been compared with holographic and ruled gratings of the same specifications, and have outperformed these other types not only in terms of diffraction efficiency, but also wavefront quality and scatter. However, a holographic grating is at least in principle capable of rather low levels of scatter, so the final level of scatter depends primarily on how well the manufacturer has perfected the recording and coating techniques.

While E-beam is the technology of choice for the smaller convex gratings of the Offner spectrometer, it is not particularly well suited to producing the larger concave gratings of the Dyson spectrometer. At present, only holographic gratings can be used for that purpose. Such gratings suffer from low efficiency, unless ion-etched to produce a near-blazed profile. The process of ion-etched gratings on curved substrates is not simple; only one company worldwide offers such a service (Zeiss of Germany). Zeiss recently delivered a convex grating for the Rosetta/VIRTIS mission. However, performance results have not yet been published.

An alternative potential method for generating these larger gratings is by x-ray lithography. This method relies on scanning a very narrow slit (much narrower than the grating pitch) over the substrate and achieving a desired profile through variation in the scan speed and hence exposure time. However, this represents more of an idea than a method at this point. A tentative start has been made towards its implementation through a collaboration between JPL and Louisiana State University, but currently this is not a funded effort. If successful, the method has the potential of providing better control over the groove profile than holographic methods.

3. Progress and issues in focal plane arrays

We have considered detectors for imaging spectrometers that operate in the 400 to 2500 nm spectral range and the 8 - 12 μm spectral range. The emphasis has been on Earth observing type missions, but many of the results will be appropriate for planetary missions too. The timescale is focused on technology that will be available for implementation into imaging spectrometers in 5 years.

VNIR spectral range

Historically, the visible portion of the spectral range in imaging spectrometers has been covered using CCD technology. The main drawback of this approach has been the lack of sensitivity in the blue. Thin poly manufacturing approaches have improved the CCD performance in the blue, but additional improvement would be beneficial. Thinned backside illuminated CCDs are also available which have excellent blue sensitivity. However, the cost of the thinned devices is generally too high for most projects to afford.

Another technology being worked on currently is the p-channel CCD. The p-channel devices are more amenable to backside thinning which results in an overall sensitivity improvement as compared to thin-poly n-channel CCDs. P-channel CCDs can support quantum efficiencies that are about 2 times higher than traditional CCDs. The read noises for these devices at high readout speeds are also slightly improved as compared to high quality n-channel CCDs. Additionally, this technology has been shown to be capable of withstanding 1 Mrad TID of ionizing radiation without significant degradation (Saks, et.al. 1979). Overall, the p-channel CCDs offer significant improvement to spectrometer performance.

The traditional CCD readout is a frame transfer readout which introduces a spectral contamination into the data. During the readout process every pixel of information will move through all photosites in a column, collecting signal from each photosite along the way. To mitigate this problem, the transfer speed of the CCD must be limited to $\sim 0.1\%$ of the integration time (on the order of 50 nsec) so that the amount of spectral contamination is kept to a tolerable level. Figure 19 shows the worse case spectral contamination for a typical spaceborne imaging spectrometer implementing a fast transfer speed CCD. For this calculation it has been assumed that all pixels except the pixel of interest are viewing a 100% reflectance target. This maximizes the contamination signal gathered during the frame transfer. At low reflectance signals in the pixel of interest, the percent spectral contamination can be fairly large. However, this must be compared to the general uncertainty in the measurement ($1/\text{SNR}$) as shown in Figure 20, obtained under an identical set of inputs. As can be seen, the spectral contamination and the general uncertainty are very similar and the maximum penalty in calibration uncertainty will be about a square root of 2.

The interline transfer CCD is another technology that is available. Although this technology has high QE, it also has low fill factor such that the overall performance is at best the same as the traditional CCD. The interline transfer allows the CCD to be read out without any spectral contamination, but the low fill factor does mean that the sampling of the spectrum may be incomplete depending on layout, spot size, etc. The interline transfer structure is of a relatively fixed size so that as a pixel gets larger the percent fill factor can be improved. Given an implementation with relatively large pixels, this technology can be successfully utilized.

Another improvement in performance could be made by implementing the visible bands in Hybrid Imaging Technology (HIT). This approach allows the light sensitive portion of the detector to be fabricated using CCD approaches and the readout portion of the detector to be fabricated using CMOS technology. CMOS is a better technology for building readouts since it requires less power, produces less noise, and does not have the spectral contamination associated with frame transfer CCDs. A HIT technology approach has potential to simplify the signal chain electronics and make them more similar to the IR detector electronics. Initial HIT results are highly encouraging. For a 256×512 device operated at -40°C , the read noise floor was about 5 rms electrons at 25 kpixel/sec readout. The charge transfer efficiency was > 0.99999 and the power dissipated by the chip was < 0.5 mW. A HIT imager tailored to the imaging spectrometer requirements should provide excellent instrument performance. Further development support is needed here.

Figure 19: Worse Case Spectral Contamination

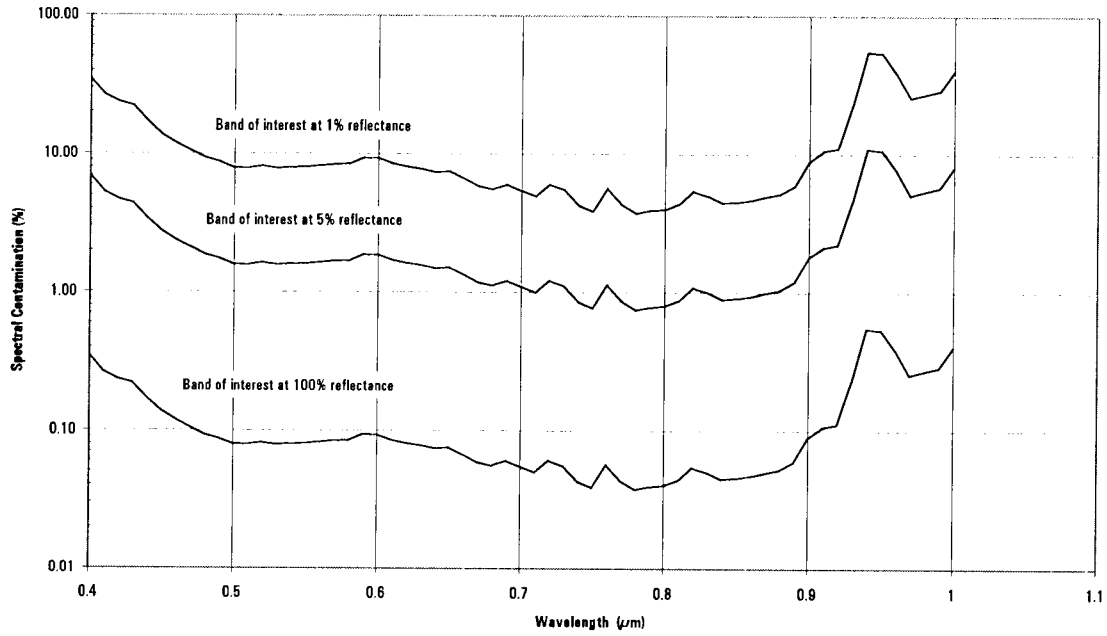
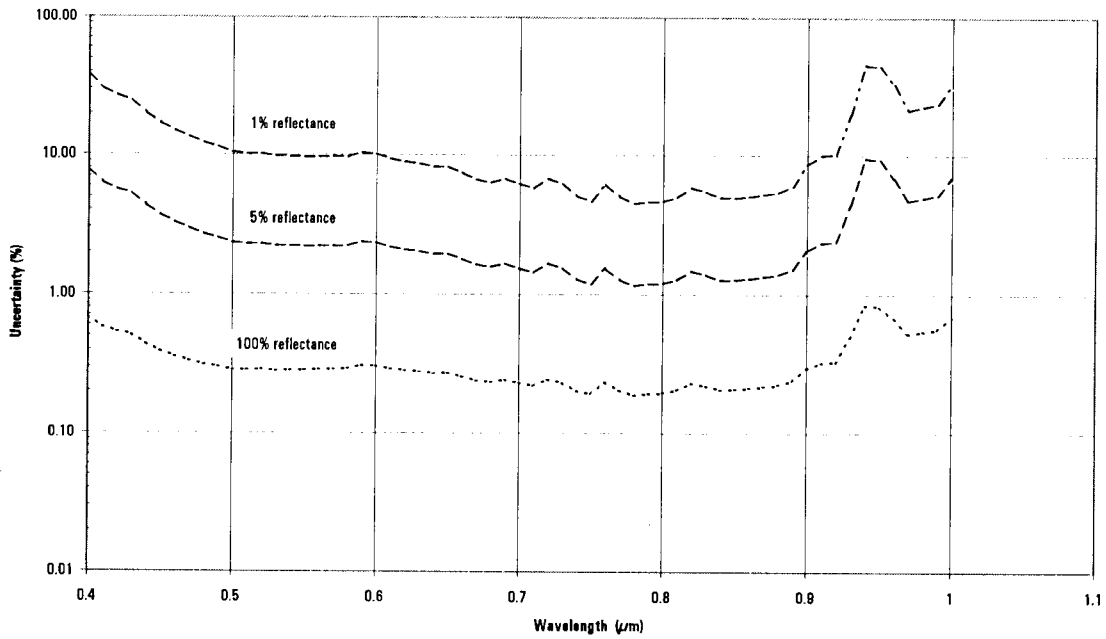


Figure 20: Measurement Uncertainty (1/SNR)



SWIR spectral range

For the SWIR spectral region (1 – 2.5 μm), most systems have implemented Mercury Cadmium Telluride (HgCdTe) or Indium Antimonide (InSb) detectors. The trade between these two technologies is mainly operating temperature and uniformity. The cutoff wavelength of HgCdTe can be tuned to different wavelengths, so that 2.5 μm cutoff HgCdTe can operate at a much warmer temperature (150-200 K), than InSb (70 -90 K). Although for many years the uniformity of InSb was clearly superior to HgCdTe, continuing development in HgCdTe has reduced this gap significantly. Uniformity here means the degree to which the response of the pixels is the same for a given flux level. A related parameter is operability and involves the number of pixels in an array whose performance meets a certain standard. Note that both materials (HgCdTe and InSb) are far less uniform in response and have lower operability than silicon. Also continuing improvement in HgCdTe manufacturing and hybridization has resulted in larger arrays of HgCdTe being available than InSb. At this time, HgCdTe is the overall best choice of detector for spaceborne imaging spectrometer due to the higher operating temperature. Airborne systems are not as driven by operating temperature concerns and InSb is still an appropriate material for such systems. Continuing work on development of warm HgCdTe technology should further improve the performance of this material.

The new silicon microbolometer technology that is being developed might be able to provide sufficient performance for implementation into imaging spectrometers. Our analysis indicates that currently available Si microbolometers are not sensitive enough for scientific grade imaging spectrometers. The maximum SNR is about 20 at high reflectance in the 1-2.5 μm range ($D^* = 1 \times 10^9$ jones; 120 Hz). However, a diode-based bolometer would have about 10 times better performance (SNR=200) which is within a factor of 3 of HgCdTe performance. This diode-based bolometer performance could be acceptable for some spectrometer implementations that can operate at long integration times (15-25 msec). The advantages of these detectors are that they can operate very warm (250-270K) for SWIR and potentially have uniformity comparable to visible silicon devices. These detectors have an extremely broad spectral range and as such the same detector technology could be used for SWIR and LWIR. There is even potential for this technology to also work in the visible. Being a silicon-based technology, larger arrays can be made, which would allow greater freedom in the optical design of spectrometers.

General Detector Issues

Most of the imaging spectrometers under discussion today utilize gratings for spectral dispersion. This requires that an order-sorting filter be placed somewhere in the system. It would be a benefit if this filter could be directly deposited on the detector. Currently, Kodak has put the most effort into this area. They have had very limited success so that the opinion of our group is that this is not going to become a viable option in the 5 year time frame and certainly would not be applicable to linear variable filter techniques.

The advent of a curved detector format would give the optical designer another degree of freedom. This sort of technology is many years in the future. However, the Navy is funding an investigation into the first steps toward a curved detector format for silicon monolithic devices. The current work seems to involve development of the projection systems for the lithography. A curved hybrid technology is even further in the future. Realistically, at this time, there is no major driver on the detector manufacturers to develop this curved detector technology. Until this driver is established, there is virtually no chance of a curved detector technology being developed. However, some of the schemes which utilize fiber optic technology to flatten a curved image plane could be useful in some applications.

As mentioned previously, uniformity of response and operability is a major issue for IR detectors. There is one technique that can improve the uniformity of response, but the cost is fairly high. The technique involves subdividing the pixels and only using the best subpixels. For example, if the pixel is divided into four subpixels, only the three best subpixels would be connected. This technique requires much a larger amount of electronics and also involves the loss of detector area, as such, it should only be considered when everything else has failed.

There is considerable flexibility in detector and pixel size for the VNIR region that is based on more mature technologies. The same cannot be said for the SWIR. Detector size for the SWIR is the limiting factor in the number of spatial pixels that can be utilized by a single spectrometer module, and also the limiting factor in spatial sampling. Currently available HgCdTe detectors offer a maximum of 720 spatial pixels of 27 μm size. This means that the limiting detector height is about 20mm. With a custom design, it may be possible to extend that to about 25-26 mm, provided the number of spectral channels is small. However, this has not been tried as yet. Significant flexibility will be gained in optical design if larger SWIR detectors become available.

4. Progress and issues in silicon carbide technology

Background: Reflective Optical Systems

Reflective optical systems for imaging spectrometry have a number of advantages for use in space. They operate over a broader wavelength band than refractive systems. In particular, a single foreoptic and (sometimes) spectrometer optic can be made to work over the full wavelength band (400 to 2500 nm) of interest for remote sensing of solar reflected radiation. The optics can be aligned using visible light, and the result will hold at all wavelengths. Reflecting systems are inherently more radiation hard than refractive ones, and reflective systems can be designed and built to have stable optical performance over a wider temperature range than refractive systems.

Advances in optics technology over past 10-15 years have expanded the range of application of reflecting optical systems. Reflective optical design forms working at higher optical speeds (low f-numbers) and over wider field angles with diffraction limited image quality over the full wavelength band of interest are now possible for applications where only refractive designs could be considered before. Further, these systems can be designed without any central obscuration so that the performance degradations due to diffraction spreading induced by central obscurations in traditional reflective optics designs can be removed. Advances in optical fabrication and test technology during the same time period mean that the off-axis aspheric mirrors required by these new designs can be made, tested, assembled, and aligned.

Traditional reflective optical systems have been made with glass mirrors and metal structures. Many systems of this type have been made to operate at high standards of performance even in the severe environments encountered in space. Glass mirrors are still used when diffraction limited performance at visible and UV wavelengths are needed. Such systems have a number of complexities, however. They are mechanically and thermally complex to design and build. The glass to metal interfaces required to mount the mirrors are complex and subject to thermal and vibration-induced stresses that jeopardize the survival or optical quality of the mirror surfaces. Complex linkages involving different metal and nonmetal materials are needed to maintain optical performance over wide temperature excursions. Finally, there is a practical limit to the degree to which glass mirrors can be lightweighted while retaining their optical figure for large aperture optical systems.

Monolithic optical systems have been explored in an attempt to overcome some of the problems of traditional metal-and-glass reflective optical systems. These systems have both the mirrors and their supporting structure made of the same material so that they are inherently compensated for bulk changes in instrument temperature. Metal mirrors can be lightweighted to a greater degree than glass ones and simpler mechanical design and construction is possible since metal-to-glass interfaces are eliminated. A more subtle advantage is that optical correction holds over wider temperature range for monolithic systems. CTE values are often unknown at extreme temperatures, but they change together in a monolithic system so as to maintain optical performance. The thermal expansion properties of glasses and metals do not necessarily change in a similar way at extreme temperatures, and thermal compensation of such systems can therefore fail at these extremes.

Up until the past 5 to 10 years, monolithic optical systems were primarily made out of aluminum. Aluminum is relatively inexpensive, and the mirror surfaces can be diamond turned to adequate surface quality for IR or longer wavelengths. Monolithic reflecting optical systems made of aluminum are widely and successfully used for a number of applications, but aluminum optics have certain limitations when it comes to producing diffraction limited optical performance at visible or shorter wavelengths in extreme environments. Aluminum mirrors must be nickel coated and post-polished to make diffraction-limited surfaces for visible applications. The bimetallic effects at the nickel/aluminum mirror interface limit the temperature range over which diffraction-limited operation can be maintained. Furthermore, material inhomogeneities inside even the best aluminum ingots coupled with the high CTE of this metal prevents diffraction-limited performance for visible systems over wide temperature ranges.

Carbon composite materials for monolithic optical systems.

A good deal of research had been made into the use of composite materials for monolithic optical systems over the past ten years or so. The most promising materials to emerge from these studies have been silicon carbide and other carbon based composite materials. Only silicon carbide will be discussed in detail in the body of this report, as it is thought to be the most promising material overall. Its unique combination of bulk material properties (high specific stiffness, low Coefficient of Thermal Expansion (CTE), and high thermal conductivity) allows it to be used to make light weight, thermally stable reflective optical systems out of one material. Proprietary composite forms of silicon carbide have been developed for making structural members that have several advantages. Complex structures can be made inexpensively out of simple shapes that require no post-processing. These composite materials are much more fracture tough than the ceramic versions of the materials, and thus offer improved mechanical damping and crack resistance.

SiC Material Properties

The combination of high specific stiffness and high thermal stability make silicon carbide a superior material for the construction of light weight, thermally stable reflective optical systems for use in space (Figure 21). Materials with high specific stiffness are both stiff and of low density. The plot in Figure 21 shows that only Beryllium is comparable to SiC in this respect. However, Be is similar to aluminum in that it has residual material anisotropies and a relatively high CTE. These properties combine to keep Be from being suitable for cryogenic visible quality applications. Beryllium is also significantly more expensive than SiC and can be obtained from only one certified vendor. Materials with high thermal stability have both high thermal

conductivity and low rates of thermal expansion. Figure 21 shows that SiC is unrivaled in this respect.

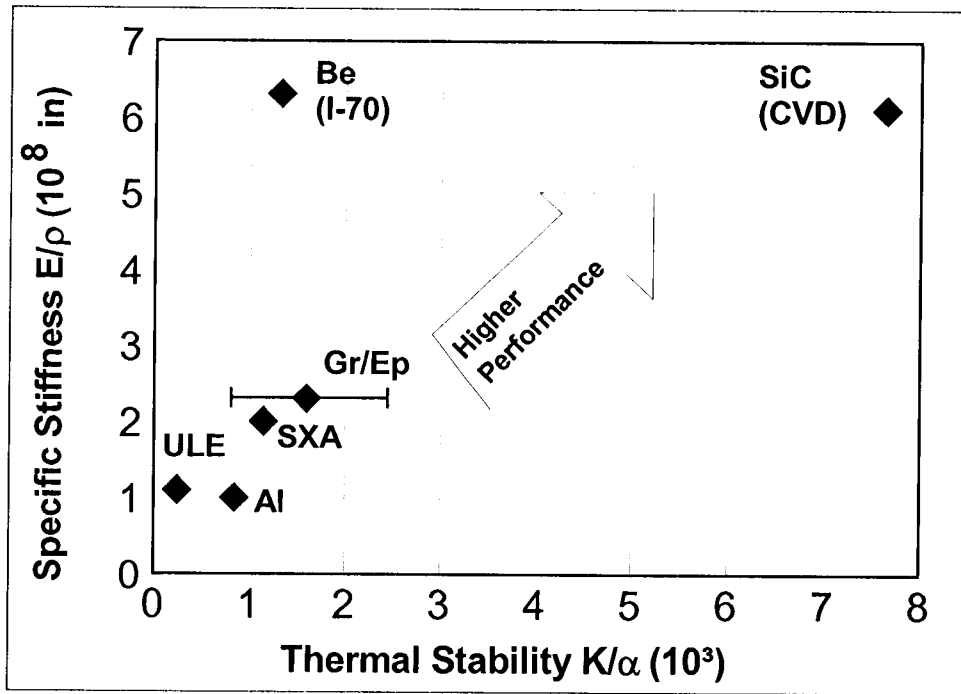


Figure 21. Candidate Mirror Bulk Material Properties (courtesy of SSG Inc.)

Figure 22 shows that SiC telescopes can be manufactured to much lower masses than aluminum telescopes of the same aperture diameter. The advantage becomes greater as the aperture size of the telescope increases.

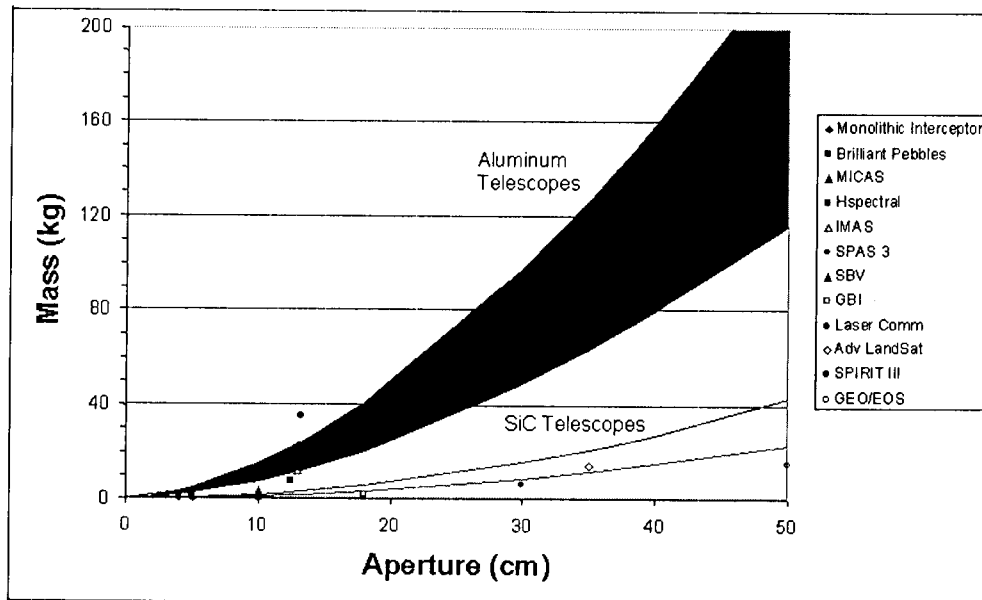


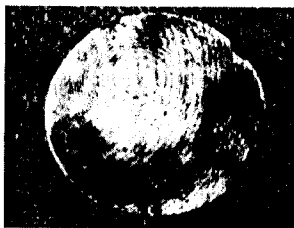
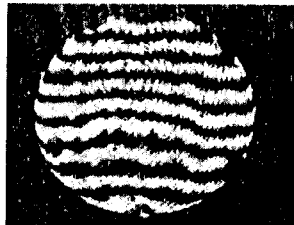
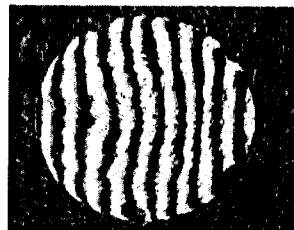
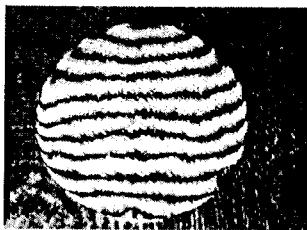
Figure 22. Telescope weight versus aperture for Aluminum and SiC (courtesy of SSG Inc.)

Ceramic grade forms of SiC

Three forms of ceramic grade SiC are available. Hot pressed SiC is made by applying high temperature and pressure to a mold of SiC particles. Chemical Vapor Deposited (CVD) SiC is grown onto a graphite base via a chemical reaction in a mixture of gases. Reaction Bonded (RB) SiC is formed from a slurry of SiC powder and water that is dried to a "green state" and then turned to hard SiC by a sequence of two furnacing operations. CVD SiC has the best bulk material properties, but is expensive to fabricate and cannot be made in lightweighted geometries directly. Areal densities of 30 to 50 kg/m² are typical for meter class sized mirror substrates made of CVD SiC. Hot pressed SiC has good bulk properties, but can only be made in simple slab shapes. Both CVD and hot pressed SiC can only be turned into light weighted, ribbed substrate shapes by machining of the hard SiC material. This machining step is not only very time consuming and expensive, but it also tends to create cracks in the semi-brittle material that can increase scrap rate. The RB SiC slurry can be formed into intricate, ribbed, light weighted shapes directly in the mold, and is thus the most promising of the three ceramic forms for making light weighted mirror substrates. 8 kg/m² areal densities have been achieved for 0.25 m class mirror substrates. Thermal testing of RB SiC mirrors have shown excellent thermal stability down to 135 K (Figure 23).

Spheres and flats of good optical quality can be made by direct polishing of the ceramic SiC surfaces. All aspheric mirrors, however, require localized hand polishing that cannot be done effectively at the moment on hard SiC surfaces. A thin layer of silicon (Si) is clad to the SiC surface to provide a softer polishing layer for the production of high quality aspheric mirrors. Si is well matched to SiC in its thermal properties, and excellent cryogenic wavefront stability has been measured for Si clad SiC mirrors.

T = 135 K
p-v WFE = 0.53 λ
rms WFE = 0.08 λ



T = 295 K
p-v WFE = 0.47 λ
rms WFE = 0.08 λ

Figure 23. Cast SiC Mirror (courtesy of SSG Inc.)

The Miniature Integrated Camera and Spectrometer (MICAS) instrument was launched on the first Deep Space New Millennium mission (NMP-DS1) in October 1998. A picture of it is shown in Figure 24. It is the first all SiC optical system to fly in space. Its structure and mirrors are made of hot pressed SiC. It also contains a small composite SiC optical bench for the IR spectrometer channel.

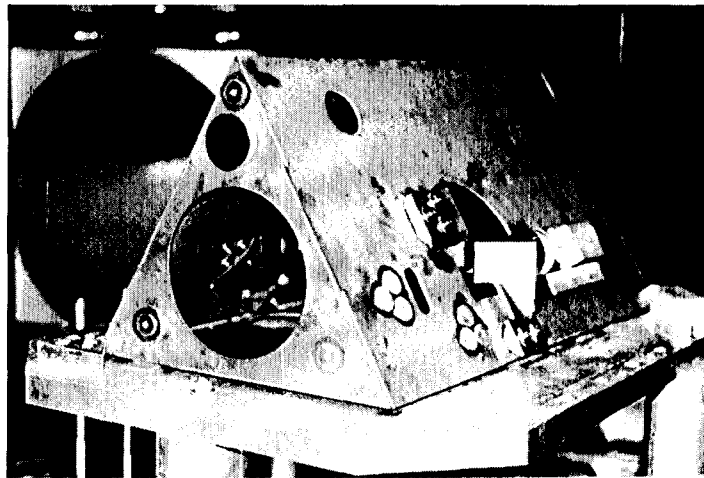


Figure 24. Miniature Integrated Camera and Spectrometer (courtesy of SSG Inc.)

Composite forms of SiC

Composite forms of silicon carbide are made out of either fabrics (SSG's SiC/SiC) or a felt material (IABG's C/SiC) using proprietary methods. These materials have the same CTE as the ceramic forms of SiC. Since they start in a pliable form that is easy to form or machine into complex shapes, they are excellent for use in building complex structural shapes and very light weight mirror substrates. The nature of these materials also makes them more fracture tough than ceramic materials and provides them with a measure of vibration damping that makes them better suited to bearing mechanical loads and withstanding launch vibrations. The use of these materials for making mirrors is still in its infancy, though the Germans have demonstrated high quality mirrors using a thin facesheet of glass bonded to the surface of the material. There are many voids in composite materials that must be filled to provide a smooth surface layer that can be polished to a mirror surface if a surface face sheet or cladding layer is to be avoided.

Two breadboard optical systems using composite SiC structures and ceramic SiC mirrors have been made for JPL by SSG, Inc. The first (Figure 25) is a laser communications telescope made under a Phase II SBIR. The second was a technology demonstration for the Integrated Multispectral Atmospheric Sounder (IMAS) (Figure 26). Both systems showed excellent stability in optical performance down to cryogenic temperatures. The IMAS system also passed vibration testing to load levels anticipated for an ELV class launch.

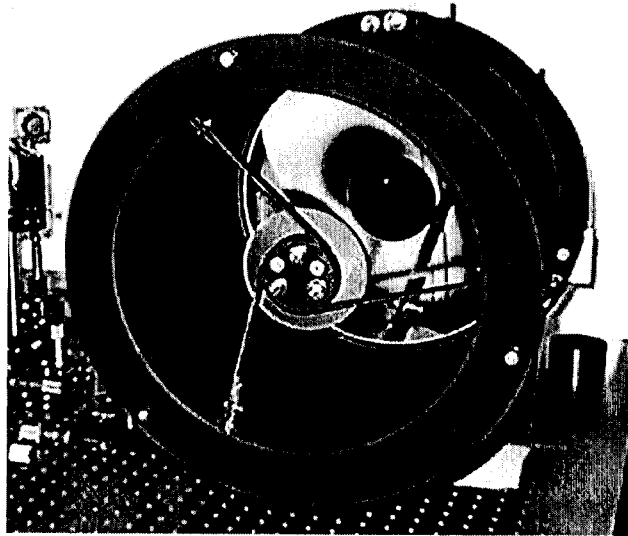


Figure 25. Laser communication SiC system (courtesy of SSG Inc.)

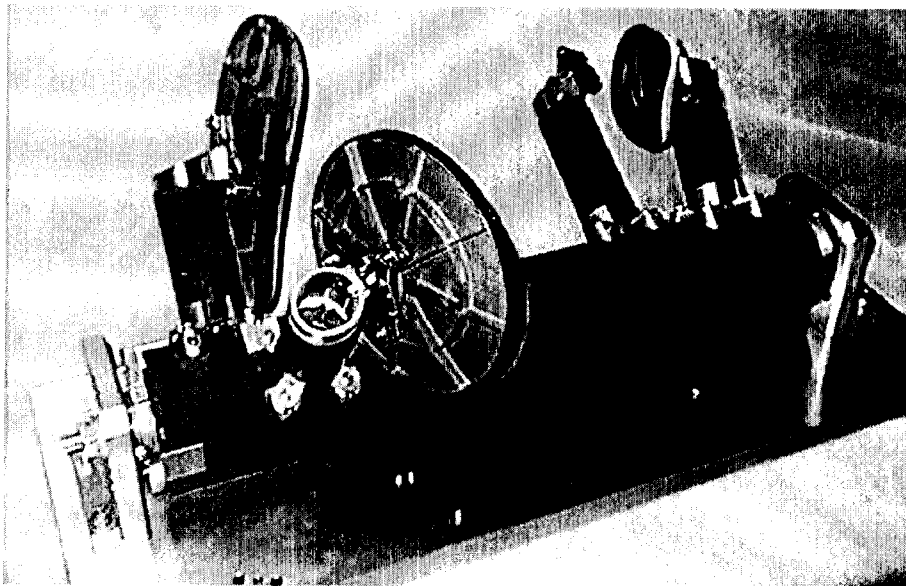


Figure 26. IMAS Mirror (courtesy of SSG Inc.)

Needed technology development for the next 3 to 5 years:

1. Improving the cost and schedule for SiC optical systems. SiC technology has advanced rapidly over the past 3 to 4 years, and cost-effective approaches for both lightweight mirrors and structures have been developed over that time. As processes are further developed, costs should continue to come down. The castable (RB) and composite forms of SiC show the best promise at

the moment for low cost and large aperture size. All of the ceramic forms of SiC are useful for small to moderate sized optics.

2. Mirror surface quality improvement. The challenge is to learn how to make powered aspheric mirrors on SiC substrates having diffraction-limited surface figure at visible wavelengths. These surfaces must not only have 1/8th wave class surface figure, but must also be low scatter surfaces. The latter requirement means that they must have residual mid-frequency ripple and microroughness errors that are comparable to glass mirrors. The solution must be cost effective to also meet the first goal above. This problem must be solved for small, moderate, and large sized mirrors. New techniques for characterizing optical system performance for figure and alignment may be needed to meet these goals cost effectively. Adaptation of the prescription retrieval methods used to diagnose residual fabrication and alignment errors on the Hubble Space Telescope (HST) might be useful as a ground based diagnostic tool in this regard. Initial studies have already been made using the MICAS and IMAS silicon carbide optical systems.

5. Progress and issues in fiber optics

A fiber bundle for reshaping a curved line image into a straight one has been described in Sec. III. Fabrication of this bundle is considered within the current state of the art. During the past year, a similar but more complicated fiber structure was developed by a private industrial company through a JPL-sponsored effort. This effort was directed at making several adjacent 120° layers of 1024 fibers each, and reformatting each one layer into a 16 x 64 rectangular array with a specified core-to-core distance (not densely packed).

Figure 27 shows an example of a fiber bundle (one layer only). The effort was successful within the tolerances of the project, but further refinement would be needed to achieve arrays with zero imperfections. However, the requirements for a hyperspectral imager with a fiber link between front optics and spectrometer are simpler. A maximum of four curved fiber layers need be used, and the output end must be formed into a straight line array with the fibers in contact. It is expected that the latter simplification will suffice to ensure a bundle with zero defects.



Figure 27. An arc-to-rectangle fiber array. The arc is ~120° (courtesy of Canadian Instrumentation and Research Ltd.).

The fibers used for this bundle had a core diameter of $\sim 50 \mu\text{m}$ and outside diameter of $\sim 64 \mu\text{m}$. This shows that light loss from the cladding/jacket area is an acceptable 39%. These fibers are fused silica core with a light doping that should withstand radiation exposure, as well as be capable of transmitting over the entire VNIR/SWIR range. However, one of the remaining issues is the careful selection of space qualified materials for construction of the bundle and adaptation of techniques as needed to accommodate such materials.

A final issue is the development of techniques for end polishing. In order to minimize light loss and avoid pupil mismatch, it is necessary to polish all fiber ends parallel to each other within a tight tolerance of less than 1° . This seems to require only proper engineering rather than new technology development.

6. Summary of important technology issues

The following technology issues have been identified as important for the further development of the next generation hyperspectral imagers from space. These are given here without any accompanying detail.

- Development of calibration methods suitable for high-performance pushbroom imaging spectrometers
- Production and testing of aberration-balancing E-beam convex gratings
- Exploration and experimental verification of Dyson spectrometer performance
- Testing and/or development of blazed concave grating fabrication methods by holographic or X-ray techniques
- Translation of remaining spectral and spatial uniformity requirements into optical parameters suitable for automatic optimization
- Design and production of low f-number ($f/1$) unobscured telescope systems
- Polishing techniques for fiber bundles that ensure parallelism of output beams
- Space qualification of materials used in fiber bundles
- Improvement in IR detector uniformity and operability
- Greater flexibility and choice in IR detector array and pixel size.
- Cost and schedule for SiC structures and mirrors.
- SiC mirror surface quality improvement.

Although this may look like a long list, it is worth remembering that in most cases the improvements sought are incremental, and that none of the remaining more substantial developments are indispensable for implementation.

V. Conclusions

- A standard set of performance requirements for pushbroom imaging spectrometers capable of generating AVIRIS-caliber science data from space has been generated.
- Imaging spectrometer systems are feasible with substantially higher performance and wider FOV than currently implemented or planned by NASA and other agencies.
- Three next-generation imaging spectrometer point designs have been shown.
- With modest development effort, critical enabling technologies will be available to support the launch of any of the point designs within the next 3-5 years.

Acknowledgments

This work was performed at the Jet Propulsion Laboratory, California Institute of Technology, under a contract with the National Aeronautics and Space Administration. Partial financial support has been provided by the Earth Science Technology Office at GSFC.

We are pleased to acknowledge J. Robichaud of SSG, Inc for his assistance in assembling information on SiC mirrors.

REFERENCES

- Green, R. O. (1998): "Spectral Calibration Requirement for Earth-Looking Imaging Spectrometers in the Solar Reflected Spectrum", *Applied Optics*, **37**, 683-691.
- Green, R. O., M. L. Eastwood, C. M. Sarture, T. G. Chrien, M. Aronsson, B. J. Chippendale, J. A. Faust, B. E. Pavri, C. J. Chovit, M. Solis, M. R. Olah, O. Williams (1998): "Imaging Spectroscopy and the Airborne Visible/Infrared Imaging Spectrometer (AVIRIS)", *Remote Sensing of Environment* **65**, 227-248.
- Mouroulis, P. (1998): "Low distortion imaging spectrometer designs utilizing convex gratings", *International Optical Design Conference 1998*, *SPIE Proc.* **3482**, 594-601.
- Mouroulis, P. and D. A. Thomas (1998): "Compact, low-distortion imaging spectrometer for remote sensing", *Imaging Spectrometry IV*, *SPIE Proc.* **3438**, 31-37.
- Mouroulis, P., D.W. Wilson, P. D. Maker, and R. E. Muller (1998): "Convex grating types for concentric imaging spectrometers", *Applied Optics* (in press).
- Saks, N.S., J. M. Killiany, P. R. Reid, and W. D. Baker (1979): "A radiation hard MNOS CCD for low temperature applications", *IEEE Trans Nuc. Sci.* **NS-26**, 5074-5079.